Possible violation of the equivalence principle by neutrinos

A. Halprin and C. N. Leung
Department of Physics and Astronomy, University of Delaware, Newark, Delaware 19716

J. Pantaleone
Department of Physics and Astronomy, University of Alaska, Anchorage, Alaska 99508
(Received 4 December 1995)

We consider the effect of a long-range, flavor-changing tensor interaction of possible gravitational origin. Neutrino-mixing experiments provide the most sensitive probe to date for such forces—testing the equivalence principle at levels below 10^{-20}. Here we justify and generalize a formalism for describing such effects. The constraints from neutrino-mixing experiments on gravitationally induced mixing are calculated. Our detailed analysis of the atmospheric neutrino data confirms a remarkable result: the atmospheric neutrino data imply the same size violation of the equivalence principle as do the solar neutrino data. Additional tests of this suggestive result are discussed. [S0556-2821(96)06310-2]

PACS number(s): 04.80.Cc, 14.60.Pq

I. INTRODUCTION AND OVERVIEW

All experiments sensitive to solar neutrinos have measured a flux of electron neutrinos smaller than that predicted by various solar models [1–3]. It is widely accepted that the solar neutrino deficit is a result of neutrino flavor mixing. The popular mechanism for this mixing is ascribed to nondegenerate neutrino masses and the inequivalence of the neutrino weak and mass eigenstates [4]. A great many studies have been devoted to deriving constraints on the mixing parameters: Δm^2, the neutrino mass-squared difference, and $\sin^2 2\theta$, the mixing angle, from the solar neutrino data.

In this paper we consider an alternative mechanism of neutrino mixing in which the flavor-changing interaction is assumed to be gravity [5,6]. This assumed violation of the principle of equivalence by neutrinos will lead to flavor mixing, even if the neutrinos are massless. Consequently, data from neutrino-mixing experiments can be used to test how well the equivalence principle is obeyed by neutrinos. As will be seen, current data probe the equivalence principle to a suprisingly stringent level.

In addition to solar neutrino experiments, recent studies of atmospheric neutrinos [7–10] also point to the existence of neutrino mixing. It is rather intriguing to note that, in contrast to the conventional mass mixing mechanism, the gravitationally induced mixing mechanism can account for the combined solar and atmospheric neutrino data by assuming *only* $\nu_e - \nu_\mu$ mixing. In the remainder of this paper we shall discuss the phenomenological consequences of such a flavor dependent gravitational interaction of the neutrinos.

We begin in Sec. II with a discussion of how neutrinos probe for flavor dependence in long-range forces. We start with the time delay in a gravitational field for a massless particle and its previous applications to photons and neutrinos. Next is a discussion of how this same time delay, if flavor dependent, can produce neutrino oscillations. Then our formalim is presented; first for massless neutrinos and then for massive neutrinos. When nonzero neutrino masses are included into our formalism, we find a new physically significant phase parameter. We conclude Sec. II with a discussion of the ambiguities of the formalism, and how some of them can be avoided. In Sec. III we summarize the constraints from accelerator and solar neutrino data; and we present a result for the atmospheric neutrino anomaly. Also, the parameter regions that planned experiments can probe are estimated. In Sec. IV we compare the allowed parameter regions obtained in Sec. III and find the remarkable result that atmospheric and solar observations both select the same, small parameter region for equivalence principle breaking. We discuss more stringent tests of this radical idea and mention some possible outstanding theoretical questions that it generates.

For those readers disinclined to move beyond the orthodoxy of metric theories of gravitation, which preserve the equivalence principle, the results presented here can be used to set the most restricive bound to date on the validity of the equivalence principle. They can also be reinterpreted as evidence for the existence of a very long-range, flavor-changing tensor interaction of gravitational strength.

II. FOUNDATIONS AND FORMALISMS

A. Time delay of massless particles in a gravitational field

The most familiar tests of the weak equivalence principle (WEP) are experiments of the Eötvös-type [11] which measure the gravitational acceleration of macroscopic objects. Currently, it is found [12] that gravity accelerates all macroscopic objects at the same rate to an accuracy of one part in 10^{12}.

A test of the WEP for massless particles stems from Shapiro's observation that the transit time for a photon traversing a given distance in a gravitational potential, $\phi[\mathbf{r}(t)]$, is dilated by the amount [13]

$$\Delta t = -(1+\gamma)\int \phi[\mathbf{r}(t)]dt, \tag{1}$$

where γ is a parameter in the parametrized post-Newtonian (PPN) formalism [14] and the integration is from the time of emission of the photon to when it is detected. In general

relativity, $\gamma=1$ and radar ranging experiments [15] have verified this prediction. In alternate theories of gravity encompassed by the PPN formalism and satisfying the WEP, γ need not equal unity, but it must be the same for all particles. Thus observation of different γ values for two different particle species would constitute a violation of the WEP. Limits on such a violation have been obtained from supernova SN1987A by comparing the arrival time of photons and neutrinos with the result [16,17],

$$|\gamma_\gamma-\gamma_\nu|<\text{few}\times 10^{-3}. \tag{2}$$

In the same way, comparing neutrinos with antineutrinos yields [18,19]

$$|\gamma_{\nu_e}-\gamma_{\bar{\nu}_e}|<10^{-6}. \tag{3}$$

B. Neutrino oscillations from flavor dependent γ-values

As a prelude, we remind the reader of the famous COW (Colella, Overhauser, and Werner) experiment [20]. In this experiment, a beam of neutrons is passed through a beam splitter and the separated beams are sent through two spatial regions that are gravitationally inequivalent. Through this passage the two beams acquire a phase difference determined by integrals of the gravitational potential through which they pass. The split beams are reconstituted and the diffraction pattern resulting from the gravitationally acquired phase difference is observed.

Similary, if γ_ν is flavor dependent, then different neutrinos will undergo different gravitational time delays when passing through the same gravitational potential and thereby acquire different phase shifts. These phase shifts are observable owing to the difference in the particle bases that diagonalize the weak and the gravitational interactions. For instance, in the case of two neutrino flavors, the weak basis (ν_e,ν_μ) may be related to the gravitational basis (ν_1,ν_2) as

$$\begin{pmatrix}\nu_e\\ \nu_\mu\end{pmatrix}=\begin{bmatrix}\cos\theta_G & \sin\theta_G\\ -\sin\theta_G & \cos\theta_G\end{bmatrix}\begin{pmatrix}\nu_1\\ \nu_2\end{pmatrix}, \tag{4}$$

where θ_G is the mixing angle. As a consequence, a ν_e will be able to oscillate into ν_μ. (It should be stressed that this oscillation will take place even if the neutrinos are massless.) More specifically, assuming plane wave propagation and a constant potential, the phase difference due to the time delay acquired by neutrinos of energy E traversing a distance l is

$$\delta_t=(\gamma_1-\gamma_2)\phi lE. \tag{5}$$

This phase shift was first described by Gasperini [5] in terms of a nonuniversal gravitational red shift. However, this result does not include the contribution of phases from the spatial part of the wave function. In order to combine these two effect in a systematic way, a more specific model is required. Such a model was considered for spinless neutrinos [6]. For completeness, we extend that discussion explicitly to the spin-1/2 case below [21].

In the absence of nongravitational interactions, the properties of a spin-1/2 particle in a specified gravitational field, $G_{\alpha\beta}$, are usually described to first order (linearized theory) by the interaction Lagrangian density [22]

$$\mathscr{L}_{\text{int}}=i\frac{f}{4}G^{\alpha\beta}[\bar{\psi}\gamma_\alpha\partial_\beta\psi-(\partial_\alpha\bar{\psi})\gamma_\beta\psi], \tag{6}$$

where $f=\sqrt{8\pi G_N}, G_N$ is Newton's constant and the metric of flat space is $g_{\alpha\beta}=(+1,-1,-1,-1)$. For our purpose, we postulate an interaction of the above form but one which allows the neutrinos ν_1 and ν_2 to couple to gravity with different strengths f_1 and f_2.

This breakdown in universality of the gravitational coupling strength destroys the symmetry that keeps the graviton massless [23]. Currently, no attractive theories have been proposed which can break the equivalence principle and yet keep the graviton massless in order to reproduce the experimental result for the deflection of light [24]. However, such a theory may be possible [25], and it has been shown that a theory with mixed massless and massive gravitons can be made consistent with all the observations [26]. Since the purpose of the model discussed here is only to put together the neutrino's temporal and spatial phase shift differences, and since the graviton mass is not directly relevant to the neutrino phenomenology, we put aside the formidable question of the complete consistency of such a theory.

The postulated interaction leads to the equations of motion for the *massless* neutrino fields, ν_j,

$$\left[\left(g^{\alpha\beta}+\frac{f_j}{2}G^{\alpha\beta}\right)\gamma_\alpha\partial_\beta+\frac{f_j}{4}(\partial_\alpha G^{\alpha\beta})\gamma_\beta\right]\nu_j=0,\quad j=1,2,\ldots. \tag{7}$$

We limit our discussion to situations in which $G^{\alpha\beta}$ varies very slowly on a scale of order the neutrino Compton wavelength, and therefore drop the terms involving a derivative of $G^{\alpha\beta}$. In this case, we readily find that the ν_j satisfy a Klein-Gordon equation,

$$(g^{\alpha\beta}+f_jG^{\alpha\beta})\partial_\alpha\partial_\beta\nu_j=0, \tag{8}$$

where $O(G^2)$ terms have been dropped for consistency with a linearized theory. We assume the gravitational field is determined by a static macroscopic matter distribution in the harmonic gauge. (Since general covariance is broken, the result will in fact be gauge dependent.) Such a field is given in terms of the Newtonian potential ϕ by [27]

$$G_{\alpha\beta}=2\phi\delta_{\alpha\beta}/f, \tag{9}$$

where $\phi(\infty)\to 0$.

We note from Eqs. (8) and (9) that the presence of the gravitational field modifies the flat space metric in a neutrino species dependent way such that, for ν_j,

$$g_{\alpha\beta}\to\left(g_{\alpha\beta}+\frac{2f_j}{f}\phi\delta_{\alpha\beta}\right). \tag{10}$$

Comparing this with Eq. (1.1) in Ref. [28] (note that ϕ is defined to be positive in Ref. [28]), we see that our approach amounts to the case in which the PPN parameters α and γ are identical and the parameters f_j are related to the PPN parameters by

$$f_j=f\gamma_j. \tag{11}$$

To illustrate the essential properties of the resulting phase shifts, we consider the case of constant ϕ, where we have the energy-momentum relation

$$E^2(1+2\gamma_j\phi)=p^2(1-2\gamma_j\phi). \tag{12}$$

To first order in ϕ, the energy eigenvalues of the neutrinos, ν_j, having the same momentum are given by

$$E_j=(1-2\gamma_j\phi)p. \tag{13}$$

For the simple case of two neutrinos, this implies that, after traversing a distance l, the two components, (ν_1,ν_2), of a state ν_e will develop a phase difference of $\delta=2(\gamma_1-\gamma_2)\phi lp$. If we revert to a description of the oscillation phenomenon utilizing states of equal energy but differing momenta, the phase difference becomes, to first order in ϕ,

$$\delta=2(\gamma_1-\gamma_2)\phi lE, \tag{14}$$

which is twice that obtained from the Shapiro effect alone.

If we compare this phase shift with that obtained in the well known case of vacuum oscillations induced by a neutrino mass difference, we find that they are related by the formal connection,

$$\frac{\Delta m^2}{2E}\rightarrow 2E|\phi|\Delta\gamma, \tag{15}$$

where $\Delta\gamma\equiv\gamma_2-\gamma_1$. By analogy, the ν_e survival probability after traversing a distance l is given by

$$P(\nu_e\rightarrow\nu_e)=1-\sin^2 2\theta_G\sin^2\frac{\pi l}{\lambda}, \tag{16}$$

where λ is the oscillation length which is here given by

$$\lambda=6.2\ \ \mathrm{km}\left(\frac{10^{-20}}{|\phi\Delta\gamma|}\right)\left(\frac{10\ \ \mathrm{GeV}}{E}\right). \tag{17}$$

Thus, in sharp constrast to the case of oscillations induced by a neutrino mass difference where λ grows with energy, gravitationally induced oscillations are characterized by an oscillation length that diminishes with increasing neutrino energy. The two mechanisms may therefore be distinguished by measuring the neutrino energy spectrum [29–31].

C. Neutrino oscillations from both gravity and mass terms

In the preceding discussions we have described how neutrino mixing is generated by breaking the equivalence principle. It is important to note that this mixing may not preclude the generation of neutrino mixing from vacuum mass terms—which is the more commonly discussed source of neutrino mixing. It is possible that there is flavor dependence in both the neutrino mass matrix and in the gravitational coupling matrix, simultaneously. This possibility has been discussed in the literature [28,31,32]. However, these discussions have overlooked an important point which we explain now.

For simplicity, we shall assume there are only two neutrino flavors. Choosing to work in the basis which diagonalizes the charged lepton mass matrix, the evolution of neutrino flavor in a medium is described by

$$\begin{aligned} i\frac{d}{dt}\begin{pmatrix}\nu_e\\ \nu_\mu\end{pmatrix}=\Bigg\{&\frac{\Delta m^2}{4E}U_M\begin{bmatrix}-1&0\\0&1\end{bmatrix}U_M^\dagger\\ &+E|\phi(r)|\Delta\gamma U_G\begin{bmatrix}-1&0\\0&1\end{bmatrix}U_G^\dagger\\ &+\frac{\sqrt{2}}{2}G_F N_e\begin{bmatrix}1&0\\0&-1\end{bmatrix}\Bigg\}\begin{pmatrix}\nu_e\\ \nu_\mu\end{pmatrix}. \end{aligned} \tag{18}$$

Here $\Delta m^2\equiv m_2^2-m_1^2$ denotes the difference in neutrino vacuum masses, N_e is the electron density of the medium, and G_F is Fermi's constant. The first term describes the contribution from vacuum masses, the second term describes the contribution from equivalence principle breaking, and the third term describes the contribution from a background of normal matter [33]. There are two unitary matrices which parametrize the mixing, U_M and U_G, and they are generally completely unrelated. The subscripts M and G denote quantities which come from the vacuum mass term and from the gravitational mixing, respectively. A general representation for a unitary matrix is given by

$$U\equiv e^{i\chi}\begin{bmatrix}e^{-i\alpha}&0\\0&e^{i\alpha}\end{bmatrix}\begin{bmatrix}\cos\theta&\sin\theta\\-\sin\theta&\cos\theta\end{bmatrix}\begin{bmatrix}e^{-i\beta}&0\\0&e^{i\beta}\end{bmatrix}, \tag{19}$$

where χ, α, and β denote arbitrary phases and θ denotes an arbitrary angle. However, not all of these phases are observable in neutrino oscillation experiments.

As is well known, when there is no gravitational mixing (e.g., in a vanishing gravitational field), all the phases in U_M may be eliminated by redefinition of the spinors, e.g., $\nu_e'\equiv e^{i2\alpha_M}\nu_e$. Then only θ_M is observable. Similarly, when the contribution from the neutrino vacuum masses is negligble (e.g., in a large gravitational field), all of the phases in U_G may be eliminated and only θ_G is observable. Thus θ_M and θ_G are each independently observable parameters. Notice that, in general, when neutrino mixing receives contributions from both the gravitational and vacuum mass terms, the χ's and β's can be eliminated but the α's cannot. Putting all of the residual phase into the gravitational term, the flavor evolution may be parametrized as

$$\begin{aligned} i\frac{d}{dt}\begin{pmatrix}\nu_e\\ \nu_\mu\end{pmatrix}=\Bigg\{&\frac{\Delta m^2}{4E}\begin{bmatrix}-\cos 2\theta_M&\sin 2\theta_M\\ \sin 2\theta_M&\cos 2\theta_M\end{bmatrix}\\ &+E|\phi(r)|\Delta\gamma\begin{bmatrix}-\cos 2\theta_G&e^{-i2\alpha}\sin 2\theta_G\\ e^{i2\alpha}\sin 2\theta_G&\cos 2\theta_G\end{bmatrix}\\ &+\frac{\sqrt{2}}{2}G_F N_e\begin{bmatrix}1&0\\0&-1\end{bmatrix}\Bigg\}\begin{pmatrix}\nu_e\\ \nu_\mu\end{pmatrix}, \end{aligned} \tag{20}$$

where $\alpha\equiv(\alpha_G-\alpha_M)$. Since this phase cannot be eliminated by redefinition of the spinors, it will have experimental consequences.

In the case of constant backgrounds (N_e and ϕ), this equation can be easily solved, yielding the oscillation probability

$$P(\nu_e,x\to\nu_\mu,y)=\frac{1}{2}\frac{a^2}{[a^2+b^2]}\{1-\cos[2\sqrt{a^2+b^2}(y-x)]\}, \quad (21)$$

where b is the diagonal element of the total mixing matrix

$$b\equiv\frac{\Delta m^2}{4E}\cos 2\theta_M+E|\phi|\Delta\gamma\cos 2\theta_G-\frac{\sqrt{2}}{2}G_F N_e, \quad (22)$$

a is the magnitude of the off-diagonal element

$$a\equiv\left|\frac{\Delta m^2}{4E}\sin 2\theta_M+E|\phi|\Delta\gamma\sin 2\theta_G e^{-i2\alpha}\right|, \quad (23)$$

and x and y denote the position of the neutrino source and detector, respectively. This solution explicitly shows that the phase is only observable when both neutrino vacuum mass mixing and gravitationally induced mixing are relevant, i.e., when Δm^2, $\Delta\gamma$, θ_G, and θ_M are all nonzero.

Phases in the vacuum mass mixing matrix may lead to violations of time reversal (T) symmetry. Under this symmetry, neutrino oscillation probabilities transform as [34]

$$P(\nu_\mu,x\to\nu_e,y)\to P(\nu_e,y\to\nu_\mu,x). \quad (24)$$

Unitarity for two neutrino flavors implies that

$$P(\nu_\mu,x\to\nu_e,y)=P(\nu_e,x\to\nu_\mu,y). \quad (25)$$

It follows that a difference in the probabilities $P(\nu_e,x\to\nu_\mu,y)$ and $P(\nu_e,y\to\nu_\mu,x)$ is a measure of T violation. However, note that the presence of a background medium may lead to an apparent T-violation, even though the underlying dynamics is T-invariant [34,35]. To avoid this one must consider a background medium which is symmetric about the midpoint of neutrino propagation, e.g., a constant background as in Eq. (21). It is then clear that the phase α does not lead to observable T violations in two-neutrino oscillations.

In summary, for two neutrinos there are two quantities which parametrize the strength at which mixing occurs, $\Delta\gamma$ and Δm^2, and three quantitites which parametrize the mixing, θ_G, θ_M, and α. Previous analyses omitted the phase α, but in a general analysis it should be included. We plan to study the effects of the phase α in more detail in a future communication.

D. Potential ambiguities

It is necessary to choose a metric in order to confront experiments. For any metric choice, breaking the equivalence principle implies neutrino mixing. However, because the particular breaking of the equivalence principle considered here also breaks general coordinate invariance, physical results depend on the choice of metric used. At present, there are few hints as to Nature's choice.

In deriving our formalism, we assumed the harmonic metric. Although this is commonly done in most discussions of $K-K$ oscillations [36], where one can test the equivalence principle between a particle and its antiparticle, the harmonic metric is certainly not the only possible assumption. For example, the authors in Ref. [21] assumed the Schwarzschild metric instead. They have obtained a neutrino oscillation formalism which only differs from ours by parameter redefinitions.

TABLE I. Values of the gravitational potential $|\phi|\equiv G_N M/r$ at various positions from various sources [70]. The Sun-Sun entry is the largest value of $|\phi|$ in the Sun due to the Sun. The details of structure on supercluster scales are not well measured at present, so there is a sizeable uncertainty in the last entry [71].

Position	Source	$\lvert\phi\rvert$
Earth	Earth	6×10^{-10}
Earth	Sun	1×10^{-8}
Solar sys.	Galaxy	6×10^{-7}
Solar sys.	Virgo cluster	1×10^{-6}
Sun	Sun	7×10^{-6}
Solar sys.	Great attractor	3×10^{-5}

Some metric choices do, however, lead to observable consequences. For instance, the oscillation wavelength in Eq. (17) is not invariant under shifts of ϕ by an overall constant. Thus the expression for ϕ that should be used in calculations is ambiguous, but this ambiguity must be resolved in order to derive phenomenological constraints. The most common procedure for fixing a definite value for ϕ is to assume that it vanishes at an infinite distance from the source. This insures that as gravity is ''turned off'' the results of special relativity are recovered. With this assumption, the local gravitational potentials due to various sources are given in Table I. We see that the value of this potential anywhere in our solar system is dominated by the mass distribution on scales larger than the galaxy. However, since the details of the structure on extragalactic scales is still a subject of investigation, the precise value of ϕ from these scales is somewhat uncertain. But it is apparent that, because the dominant ϕ comes from scales much larger than the propagation length in any current neutrino observation, it is reasonable to ignore the variation of ϕ over the solar system and to take it to be a constant—the same constant for all local neutrino experiments. Since $\Delta\gamma$ and ϕ always occur multiplied together, we can avoid the issue of the uncertainty in ϕ by calculating the constraints on the product $\phi\Delta\gamma$. Calculating the constraints in this manner has several additional advantages. For the most part, it covers the possibility that ϕ does not ''turn off'' at large distances, or that there is some ''cosmological'' value for ϕ. Also, it covers the possibility that ϕ is generated by a long-range tensor interaction other than gravity. Thus, by treating ϕ as an unknown constant for our solar system, we avoid many of the ambiguities inherent to these calculations.

We briefly mention the interesting possibility that the coupling between gravity and neutrinos might be spatially anisotropic. Such effects have been considered for photons (see, e.g., [37] and references therein). For example, the equivalence principle breaking might come from a coupling of neutrinos to $\nabla\phi$, the gradient of the gravitational potential, instead of to ϕ. This coupling exists in our formalism but its effects are expected to be drastically suppressed compared to the leading effects considered here [see the discussion after Eq. (7)]. This kind of coupling may also occur in string theories [38]. Constraints on such a coupling have been considered in Ref. [30]. An interesting consequence of this cou-

pling is that the amount of neutrino mixing depends on the orientation of the neutrino's momentum with respect to the gravitational source.

III. EXPERIMENTAL CONSTRAINTS

In this section we calculate the experimental limits on the gravitationally induced mixing (GIM) parameters, $\Delta\gamma$ and θ_G, from neutrino experiments.

A. Constraints from rare muon decays

The anomalous neutrino-gravity interaction breaks the lepton number symmetry of each family and will give rise to rare leptonic decay processes. One might expect a particularly stringent constraint to arise from the decay $\mu\to e\gamma$. Here we consider what limits are placed on the GIM parameters by this process.

The specific GIM interaction considered in the preceding section affects only neutrinos. Consequently the leading contributions to the decay $\mu\to e\gamma$ arise at the one-loop level. These contributions turn out not to be renormalizable. However, it might be argued that the equivalence principle is broken at a scale that still preserves the weak isospin symmetry. Since gravitation is not (yet) describable as a renormalizable gauge theory, the argument is suspect. Nevertheless, we shall examine this scenario, since it will generate the rare muon decay at tree level and presumably provide the most restrictive calculable constraint on the equivalence principle violating parameters obtainable from this process. While the standard model symmetry allows an additional equivalence principle violating term for the right-handed charged leptons, we shall ignore this complication. We simply replace the (left-handed) neutrino fields in their anomalous gravitation interactions by the corresponding left-handed family isospin doublets and make the derivatives appearing there SU(2) gauge covariant in the usual fashion. This leads to three tree-level Feynman diagrams which yield a decay rate of order magnitude

$$\Gamma\sim\alpha m_\mu(\Delta\gamma\phi\sin2\theta_G)^2, \tag{26}$$

where α is the fine structure constant and m_μ is the muon mass. Taking the large but somewhat uncertain value of $|\phi|=3\times10^{-5}$, we estimate the branching ratio for $\mu\to e\gamma$ to be

$$B(\mu\to e\gamma)\sim2.3\times10^{6}(\Delta\gamma\sin2\theta_G)^2. \tag{27}$$

Since the current experimental limit [39] is $B(\mu\to e\gamma)<5\times10^{-11}$, this leads to the constraint

$$|\Delta\gamma\sin2\theta_G|<5\times10^{-9}. \tag{28}$$

Except for very small mixing angle, this constraint on $\Delta\gamma$ is inferior to the constraints obtained below from solar, atmospheric, and accelerator neutrino experiments.

B. Constraints from accelerator experiments

There exist numerous constraints on neutrino mixing from experiments using neutrinos produced by accelerators. Because accelerators produce a neutrino flux which is mostly muon neutrinos with a much smaller electron-neutrino component, these experiments mostly probe $\nu_\mu-\nu_x$ mixing with a reduced sensitivity to $\nu_e-\nu_x$ mixing. Accelerator experiments typically involve neutrinos with energies ranging from a GeV to hundreds of GeV, and propagation lengths up to a kilometer. Since the neutrino cross section increases with energy, these experiments can achieve large event rates and so can probe for relatively small values of the mixing angle. Most importantly for us, the high neutrino energies in these experiments make them powerful tools for testing the equivalence principle because the gravitationally induced mixing ''turns on'' with increasing energy.

It is difficult to utilize the published analyses to obtain the exclusion region for $|\phi\Delta\gamma|$ and $\sin^2 2\theta_G$. This is because the energy dependence of GIM is so radically different from the case of mass mixing that the analyses must be completely redone. However, many important details such as the energy dependence of the observed and expected event rates are seldom published. We are thus forced to a less than optimal estimate of the exclusion region. Here we calculate the exclusion region for accelerator experiments in the long wavelength and the short wavelength limits. These lines are then extended to intersect in order to estimate the full exclusion region. The constraint in the short wavelength limit is obtained by taking the average probability at minimum sensitivity to be the same for both mixing mechanisms. The constraint in the long wavelength limit is obtained by using the minimum Δm^2 from the published analysis to calculate the typical energy scale of the experiment and, with the average length given in the published reference, we compute the minimum value for $|\phi\Delta\gamma|$. In this admittedly crude fashion, we obtain the excluded regions shown by the straight-line contours in Fig. 1. We estimate that these contours are accurate up to factors of 3 in $|\phi\Delta\gamma|$. We have selected experiments [40] having the largest values of $E\cdot l$, for they provide the most stringent limits.

Recently, the LSND accelerator neutrino experiment has reported some candidate events that may [41], or may not [42], indicate $\nu_\mu-\overline{\nu_e}$ neutrino oscillations. The favored parameter region lies above $|\phi\Delta\gamma|>5\times10^{-18}$ and so large mixing angles are excluded by other, higher energy, accelerator neutrino experiments [43]. There may be a very small parameter region, allowed by all accelerator experimental results, at $\sin^2 2\theta\approx10^{-3}$ and $|\phi\Delta\gamma|\approx2\times10^{-16}$. In light of the preliminary nature of the LSND experimental results, we shall not pursue this analysis further.

There are several serious proposals for a new generation of accelerator experiments with neutrino propagation lengths of several hundreds kilometers [44,45]. For example, the MINOS experiment would send a neutrino beam from the Fermilab accelerator to the Soudan-2 detector located 730 kilometers away. The lower, curved contours in Fig. 1 estimate the GIM parameter region that can be probed by this experiment. Note that matter effects start to become important at these longer distances and cause a difference in the neutrino and antineutrino oscillation probabilities, as shown by the solid and dotted curves in Fig. 1.

C. Constraints from reactor experiments

Numerous constraints on neutrino mixing have been obtained from experiments using neutrinos produced by nuclear

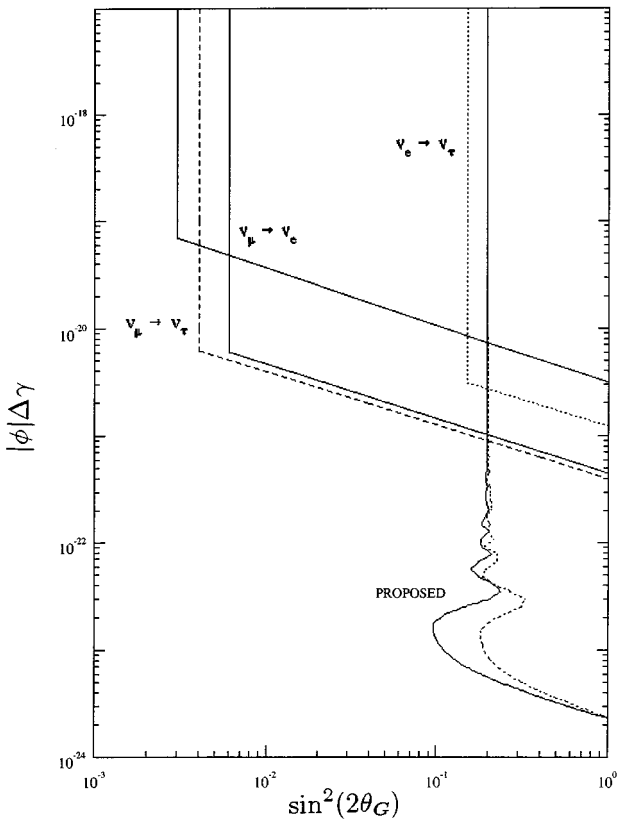

FIG. 1. Constraints on GIM parameters from present and proposed accelerator neutrino experiments. To the right of the straight-line contours lie the regions of $|\phi\Delta\gamma|$ and $\sin^2 2\theta_G$ that are excluded by current accelerator experiments (see Sec. III B and Ref. [40]). To the right of the curved contours lie the regions that may be probed by MINOS, a planned long-baseline accelerator experiment, assuming a 10% sensitivity for a disappearance experiment and $\Delta\gamma>0$. The outer, solid curve is for ν_μ while the inner, dotted curve is for $\bar{\nu}_\mu$.

reactors. Nuclear reactions create neutrinos with energies ranging from a fraction of an MeV to order 10 MeV, and these have been detected hundreds of meters from the reactors. While these relatively low energy neutrinos provide stringent constraints on mass mixing, they provide only very weak constraints on GIM because of the contrasting energy dependence of the two mechanisms. Specifically, reactor experiments only probe values of $|\phi\Delta\gamma|>1\times10^{-16}$. For the GIM mechanism, reactor constraints are completely surpassed by those from accelerator experiments, so we shall not discuss them further.

D. Solar neutrino constraints

The nuclear reactions which power the sun also produce neutrinos. These neutrinos have been observed here on Earth by several experiments [46–49]. These experiments study different ranges of the neutrino spectrum, which extends up to 14 MeV and is a superposition of several components (see, e.g. [1],). All of these measurements find far fewer neutrinos than expected (see Table II). This is commonly interpreted as evidence for neutrino mixing. This is because both the production and detection of solar neutrinos primarily involve only the ν_e flavor, so any mixing will reduce the observed flux. Here we shall assume that all of the neutrino mixing comes from the GIM mechanism, and derive the implications of solar measurements for GIM parameters.

The oscillation probabilities are calculated analytically. Here, in accordance with the discussion in Sec. II D, we shall take ϕ to be a constant (in our earlier analysis [29] we used the ϕ generated by the Sun). GIM effects start being important for solar neutrinos when $|\phi\Delta\gamma|>2\times10^{-25}$. This is when a 10 MeV neutrino undergoes half of an oscillation in its propagation from the Sun to the Earth. For larger values of $|\phi\Delta\gamma|$ the oscillation wavelength, Eq. (17), is smaller, and when the wavelength is less than the size of the Sun, the effects of the background matter become important. The analysis of matter effects [33] parallels the well known case for mass mixing [50] (for a review, see, e.g., [51]), with the substitutions of Eq. (15) (for constant potential) and $\theta\to\theta_G$. The condition for a resonance to occur is now given by

$$\sqrt{2}G_F N_e = 2E|\phi|\Delta\gamma\cos 2\theta_G, \tag{29}$$

where N_e is the electron density in the Sun. Note that when matter effects are relevant, the sign of $\Delta\gamma$ is important. For $\Delta\gamma>0$ the neutrinos can go through a resonance, and if the transition is adiabatic, large reductions in the neutrino flux occur. The calculated oscillation probability, for $\Delta\gamma>0$, is shown in Fig. 2 as a function of neutrino energy, E, times $|\phi|\Delta\gamma$. Scanning across Fig. 2 from low to high energies, we see that first the long wavelength oscillations occur, then the nonadiabatic side of the Mikheyev-Smirnov-Wolfenstein (MSW) well, and then the adiabatic side. This order is a reversal from that of the mass mixing mechanism, which provides a means to experimentally distinguish the two mechanisms.

The most recent solar neutrino data and solar model results are used in our calculation of the constraints on GIM parameters. In addition to the results given in Table II, the Kamiokande group has looked at how their data depends on energy [47]. These data can be used to constrain mixing,

TABLE II. Results of the Homestake [46], Kamiokande-II [47], and combined SAGE [48] and GALLEX [49] solar neutrino experiments.

Experiment	Process	$E(_{\text{threshold}})$	Rate (SNU)	Theory (SNU)
Homestake	$\nu_e+{}^{37}\text{Cl}\to e+{}^{37}\text{Ar}$	0.81 MeV	2.5 ± 0.3	8.0 ± 1.0
Kamiokande-II	$\nu+e\to\nu+e$	7.5 MeV	0.50 ± 0.07[a]	1.0 ± 0.15[a]
GALLEX+SAGE	$\nu_e+{}^{71}\text{Ga}\to e+{}^{71}\text{Ge}$	0.24 MeV	$78(\pm)10$	137 ± 8

[a]The Kamiokande flux is not given in SNU, but as a fraction of the standard solar model [1] prediction.

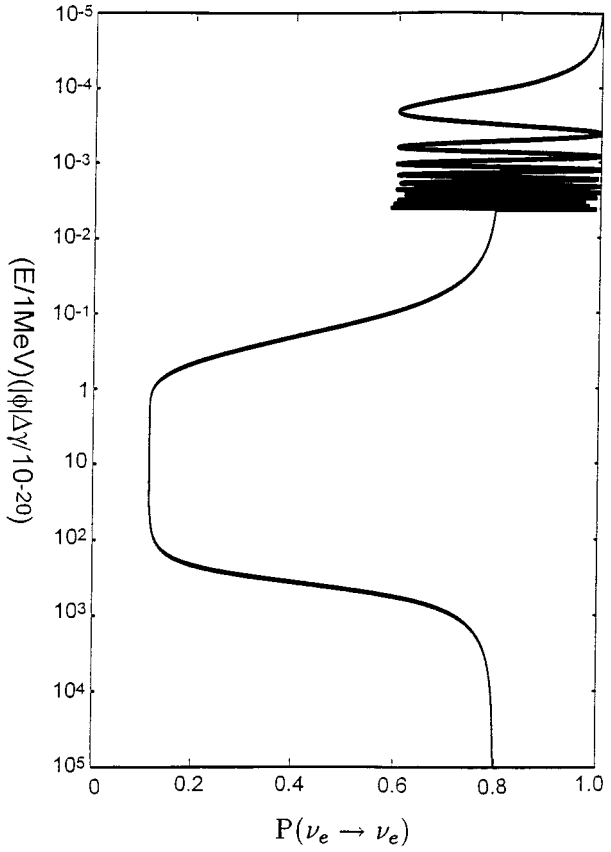

FIG. 2. Plot of $P(\nu_e \rightarrow \nu_e)$ as a function of $E|\phi|\Delta\gamma$ for $\sin^2 2\theta_G = 0.4$. The oscillation probability has been averaged over the ^{8}B neutrino production region of the Sun.

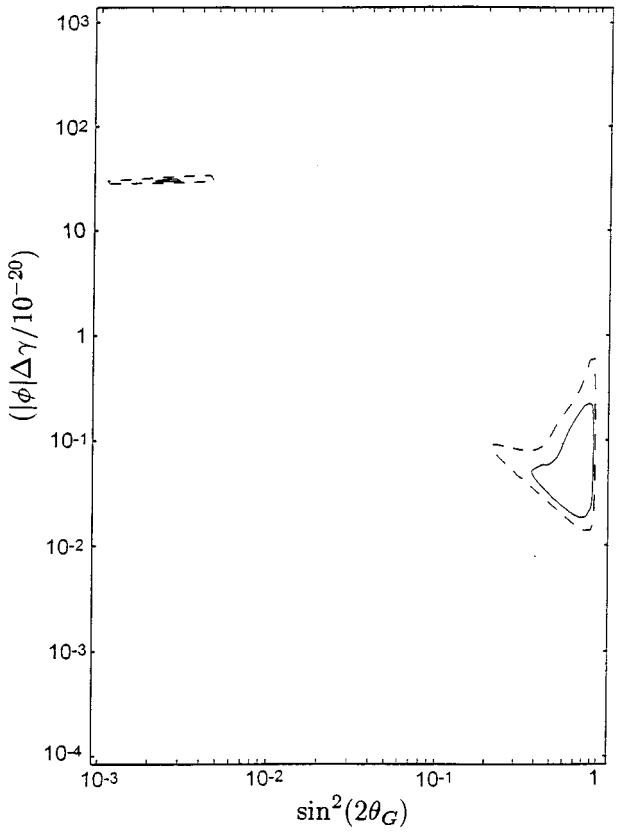

FIG. 3. χ^2 plot showing regions of $|\phi|\Delta\gamma$ and $\sin^2 2\theta_G$ allowed by the solar neutrino data in Table II at 90% (solid lines) and 99% (dashed lines) confidence level, assuming two neutrino $\nu_e - \nu_x$ mixing.

since mixing effects can be energy dependent (see Fig. 2). Much of the neutrino energy dependence is lost in the neutrino-electron scattering process, which occurs in the Kamiokande detector, but enough remains to be important. We have folded our oscillation probabilities into the neutrino spectrum and then integrated this times the cross section over energy to get the predicted result for each Kamiokande energy bin, and for each of the other experiments. The total χ^2 is calculated between the predicted and measured results and this is used to find the allowed GIM parameter regions. Only the experimental errors were included, since these are estimated to be the largest. We first calculated the allowed parameter region in the mass mixing mechanism. We then compared these calculations with those of others (e.g., [52]) and found that our 90% contours were in good agreement with theirs. We used the same value of χ^2 to calculate the corresponding 90% contours in the GIM mechanism. This insures that the mass mixing mechanism and the GIM mechanism are treated equally in fitting the same data.

The results of our analysis are given in Fig. 3. There are plotted the allowed parameter regions at 90% and 99% confidence levels, assuming $\Delta\gamma > 0$. For $\Delta\gamma < 0$ there is no allowed parameter region because then matter effects suppress mixing. The updated data, and the use of a constant $|\phi|$, do not significantly alter the allowed parameter regions from those found in our earlier analysis [29], which were independently confirmed [30]. There are two allowed parameter regions: one at large mixings, where the MSW effect suppresses mostly the intermediate and high energy neutrinos, and another at small mixings, where the MSW effect suppresses mostly the intermediate energy neutrinos. These two parameter regions are analogous to the two MSW regions found for the mass mixing mechanism (see, e.g., [52]).

For the mass mixing mechanism there is also a long wavelength, vacuum oscillation solution (see, e.g., [53]). For the GIM mechanism, long wavelenth effects are relevant for large vacuum mixings and $|\phi\Delta\gamma| \approx 2\times 10^{-25}$. Around this point only the highest energy solar neutrinos are suppressed (see Fig. 2). However, the data require some suppression at low neutrino energies so there is no allowed GIM parameter region near this value [29].

There are several new solar neutrino experiments which will test these explanations of the data. The Sudbury Neutrino Observatory (SNO) [54] experiment will definitively test all neutrino-mixing explanations of the solar neutrino deficit by performing a flavor independent measurement of the solar neutrino flux. The SNO and Super-Kamiokande [55] experiments will be able to measure the energy dependence of the high energy solar neutrino flux. The large mixing solution would not give an energy dependence observable in these experiments, but the small mixing solution would. Both of these experiments can also look for day-night variations from a resonance with matter in the Earth. These variations are large for these experiments when the mixing

angle is large and when $0.75<|\phi|\Delta\gamma/10^{-20}<2.5$. Thus, if the experiments are sensitve to small day-night variations, part of the large mixing solution may be probed by this method. In addition, the BOREXINO experiment [56] will measure the flux of Be^7 neutrinos with high statistics. This flux is almost monoenergetic so long-wavelength oscillations are important for a wide range of parameters. By looking for temporal variations on scales from a few days to a few months, correlated with changes in the Earth-Sun distance, this experiment can probe the parameter region

$$3\times10^{-4}<\frac{|\phi\Delta\gamma|}{10^{-20}}<0.3 \tag{30}$$

at large values of the mixing angles [57]. Thus BOREXINO can probe all of the large mixing angle solution. These new probes using neutral current flux measurements, spectral distortions, and temporal variations are especially important because they are independent of uncertainties in the solar model.

E. Connection with supernova dynamics

In a stellar collapse, neutrinos are created in large numbers in the hot, high density core, and then diffuse out to lower matter densities where they then freely pass through the outer layers of the star. If the neutrinos were to go through a resonant flavor conversion in the region near the supernova's core, this would have important, observable effects. Present models of supernovae suggest that this would increase the size of the explosion by about 50%, and it would also block the production of r-process nuclides [58]. The first effect would be a welcome one, since historically theoretical models have fallen short of the observed energy. However, the second effect would eliminate one of the most promising sites for r-process nucleosynthesis (see, e.g., [59] and references therein). Our knowledge of supernova dynamics is presently too sketchy to allow reliable constraints to be placed on any neutrino-mixing parameters. Here we estimate the GIM parameter region that is relevant for supernova dynamics.

Qualitatively, supernova neutrinos propagate from high to low densities just as do solar neutrinos. However, calculating the probability that a supernova neutrino's flavor survives a resonant transition is technically more difficult because the large neutrino background in a supernova makes the flavor evolution nonlinear [60]. A recent numerical study has found that this effect substantially reduces the relevant parameter region [61]. Using the results of this study, we estimate that GIM parameters in the range

$$\Delta\gamma>4\times10^{-14}, \quad \sin^2 2\theta>10^{-3} \tag{31}$$

would have substantial effects on supernova dynamics. In this estimate we took the gravitational potential at the nucleosynthesis region of a supernova to be 10^{-1}. Because this value is larger than those in Table I, we did not take ϕ to be a constant determined by external sources in deriving Eq. (31) (see the discussion in Sec. II D). To compare the parameter region relevant for supernovae with those obtained in local neutrino observations, we must multiply the above limit on $\Delta\gamma$ by the value of ϕ relevant to the solar system. Taking this to be 3×10^{-5}, the supernova parameter region lies just above the parameter region probed by the solar neutrino measurements.

F. Atmospheric neutrino constraints

Recent experimental studies [7–10] of neutrinos produced in the Earth's atmosphere have found evidence for neutrino mixing. Atmospheric neutrinos have properties very different from solar neutrinos. Atmospheric neutrinos are more energetic, with energies ranging from fractions of a GeV to several thousand GeV. Furthermore, their propagation length is shorter; it varies from 20 to 13 000 km. In the mass mixing mechanism, the oscillation phase depends on $length/energy$, so this quantity is much smaller for atmospheric neutrinos than it is for solar neutrinos. Consequently the mass mixing mechanism requires mixings of different neutrino pairs to fit the combined solar and atmospheric neutrino data (see, e.g., [62]). In contrast the oscillation phase in the GIM mechanism depends on $length\times energy$, which has the same order of magnitude for both the solar and the atmospheric neutrinos [29]. This offers the suggestive possibility that the solar and atmospheric neutrino data can be simultaneously explained with the same neutrino-mixing parameters. This expectation is indeed confirmed by the results of our analysis discussed below.

The most precise measurements of the atmospheric neutrino flux have been made with the large water Cherenkov detectors Kamiokande [7,8] and IMB [9]. These detectors each have exposures which are more than five times larger than that of any other detector. Here we confine our analysis to their results. Many quantites used in the calculation of neutrino event rates have large uncertainties. For example, the prediction for the absolute atmospheric neutrino event rates has an estimated uncertainty of about 30%. Thus one must be careful about which experimental results are used to constrain neutrino mixing. We do not use the experimental results of FREJUS [63] because of their smaller statistics, and because their results and those in Ref. [64] depend on the neutrino-rock cross section for which sizeable corrections have been calculated recently [65]. The predictions for the relative rate of events starting in the detector is believed to be much more reliable, with an estimated uncertainty of only about 5%. Neutrino mixing could change the relative number of ν_μ to ν_e in the flux from the expected value of approximately 2. Thus the relative rate can be used as an indicator of neutrino-mixing effects.

Kamiokande and IMB have both measured the ratio of ν_μ to ν_e for events fully contained in their detector. Dividing this number by the ratio predicted by a Monte Carlo analysis gives

$$R\equiv\frac{N_\mu^{\rm exp}/N_{\rm e}^{\rm exp}}{N_\mu^{\rm MC}/N_{\rm e}^{\rm MC}}. \tag{32}$$

In the ''sub-GeV'' energy range (0.3 – 1.3 GeV for Kamiokande, and 0.3 – 1.5 GeV for IMB), this ratio is found to be

$$R=0.60\pm0.05\pm0.05(\text{Kam}),$$

$$R=0.54\pm0.05\pm0.12(\text{IMB}). \tag{33}$$

Kamiokande has also measured this ratio for higher energy (1.3 GeV to around 10 GeV) neutrinos, which involve fully contained as well as partially contained events. They find this ''multi-GeV'' ratio to be

$$R = 0.57 \pm 0.07 \pm 0.07(\text{Kam}). \tag{34}$$

These consistent departures from 1.0 suggest neutrino mixing.

In addition, the Kamiokande group has studied how their data depends on the zenith angle. As the angle between the neutrino and the zenith varies from 0 to π, the neutrino propagation length varies from 20 to 13 000 km. Both mass mixing and GIM predict that mixing effects should appear at ''long'' distances, so an unusual angular dependence could indicate neutrino mixing. The cross section in the ''sub-GeV'' energy range is relatively isotropic, so no evidence for an angular dependence is expected or found in those data. In the ''multi-GeV'' energy region, the cross section is more directional, with the average angular spread between the neutrino and its associated charged lepton being $\Theta_{\text{rms}} \approx 15° - 20°$. There Kamiokande has found an angular dependence in their data, with longer path lengths associated with smaller R values [8]. This also suggests neutrino mixing.

Neutrino mixing modifies the observed event rates as given by

$$N_e = N_e^{\text{MC}}[P(\nu_e \to \nu_e) + rP(\nu_\mu \to \nu_e)],$$

$$N_\mu = N_\mu^{\text{MC}}[P(\nu_e \to \nu_\mu)/r + P(\nu_\mu \to \nu_\mu)]. \tag{35}$$

Here N_α denotes the number of charged leptons of type α observed in a particular bin, and the MC superscript denotes the number expected without oscillations from a Monte Carlo calculation. The ratio of the ν_μ flux to the ν_e flux is denoted by r and is approximately 2.1 [66]. The P's are the oscillation probablities averaged over the energy and length distributions relevant for a particular bin. In the calculations performed by the experimental groups, the data is broken up into an array of bins depending on energy and zenith angle. However, these full data arrays are not published. For our calculations, all of the sub-GeV data lies in just one bin, while the multi-GeV data is divided into five zenith angle bins.

The oscillation probabilities are calculated analytically. Here, as for the earthbound accelerator neutrino experiments and the solar neutrino measurements, ϕ is taken to be a constant (see discussion in Sec. II D). For $\nu_\mu - \nu_e$ oscillations matter effects are accounted for by using a two density (core and mantle) model for the earth, assuming $\Delta\gamma > 0$, and taking 3/7 of the data to be due to antineutrinos. The oscillation probabilities are averaged over neutrino energy distributions as given in Refs. [8] and [67]. The average over length distributions is calculated as

$$\langle P_\nu \rangle \propto \int d\Omega P_\nu(\theta) I_\nu(\theta) \int_{\text{bin}} d\Omega' P(\theta, \phi; \theta', \phi'), \tag{36}$$

where θ is the zenith angle, P_ν denotes the neutrino oscillation probability, I_ν is the neutrino flux intensity at the detector without mixing, and $P(\theta, \phi; \theta', \phi')$ denotes the probability of a neutrino with angular coordinates θ, ϕ giving rise to a charged lepton with angular coordinates θ', ϕ'. For the sub-GeV data the last quantity is not necessary, but for the multi-GeV data we take it to be a Gaussian with a rms spread of 20° [8]. For I_ν, we assume that at their production point in the atmosphere the neutrino fluxes are independent of angle and energy. This is a good approximation for the multi-GeV energy range. With this assumption, $d\Omega I_\nu$ at the detector is proportional to the particularly simple form of dL/L where L is the neutrino propagation length.

We treat the ''sub-GeV'' and ''multi-GeV'' data sets independently, because the relative errors (e.g., in the cross section, etc.) between these two energy ranges have not been studied. For each data set we calculate the χ^2 between the predicted and observed event rates [68]. In addition to statistical errors, we include a 30% error for the overall flux normalization. We do not explicitly include other, much smaller, errors in our χ^2's (e.g., those from particle misidentification, the Monte Carlo calculations, etc). Instead we first calculated the allowed parameter region in the mass mixing mechanism. We then compared these calculations to those of the Kamiokande experimental group [8], and found that our model gave 90% contours that were in good agreement with theirs for particular, reasonable choices of χ^2. We then used these values of χ^2 to calculate the corresponding 90% contours in the GIM mechanism. This procedure was adopted for several reasons: it tests our model and insures that it is reasonable and accurate, it includes as many unknown experimental effects as possible into our calculations, and it insures that the mass mixing mechanism and the GIM mechanism are treated equally in fitting the same data.

The regions of allowed GIM parameters are shown in Fig. 4. Figure 4(a) is for $\nu_e - \nu_\mu$ mixing and Fig. 4(b) is for $\nu_\mu - \nu_\tau$ mixing with $\Delta\gamma > 0$ (for $\Delta\gamma < 0$ the contours are almost identical). The parameter regions allowed by the sub-GeV and multi-GeV data sets lie to the right of the dashed and solid contours, respectively. The sub-GeV measurements are insensitive to any angular dependence in the flux, so they allow arbitrarily large values of $|\phi|\Delta\gamma$ where the oscillations completely average out. However, the multi-GeV data contains some angular dependence so it extends only over a finite range of $|\phi|\Delta\gamma$. Because higher energy neutrino experiments are more sensitive to GIM effects [see Eqs. (16) and (17)], the bottom of the multi-GeV contours lies below the bottom of the sub-GeV contours. The overlapping region is where both data sets can be simultaneously explained. For $\nu_e - \nu_\mu$ mixing, Fig. 4(a), the overlapping region is relatively large and contains the best fit points for both data sets. Thus the sub-GeV and multi-GeV atmospheric neutrino data can be consistently explained by the GIM mechanism.

There are several new atmospheric neutrino measurements which will test this explanation of the data. Super-Kamiokande [55] will increase the precision of the existing Kamiokande measurement. Soudan-2 [10] will measure the flux in a detector that is not a water Cherenkov type experiment. In addition, the next generation of neutrino telescopes [69], DUMAND, AMANDA, NESTOR, and Baikal, may be able to accurately measure the atmospheric neutrino flux at energies which are an order of magnitude larger. While the mass mixing mechanism turns off at these higher energies, the GIM explanation of the data does not. As these experiments measure the angular dependence of the flux, they will

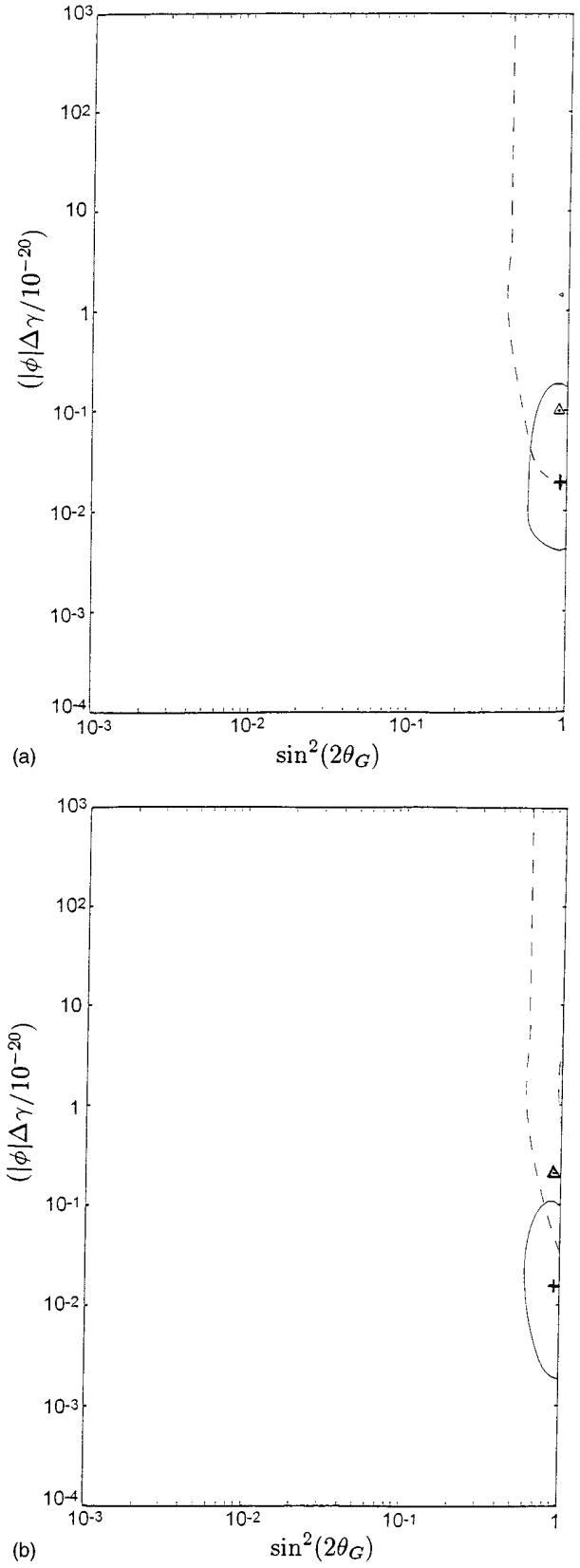

FIG. 4. Plot of $|\phi|\Delta\gamma$ versus $\sin^2 2\theta_G$ showing parameter regions allowed by the atmospheric neutrino data at 90% confidence level. Two flavor neutrino oscillations are assumed with $\nu_e - \nu_\mu$ oscillations in (a) and $\nu_\mu - \nu_\tau$ oscillations in (b). The region allowed by the sub-GeV data lies to the right of the dashed contours, and the region allowed by the multi-GeV data lies to the right of the solid contours. The best-fit points are also shown by a triangle for the sub-GeV data and a cross for the multi-GeV data.

probe a parameter region an order of magnitude below that probed by the current atmospheric neutrino experiments.

IV. DISCUSSION AND CONCLUSIONS

We have reviewed all of the present experimental constraints on neutrino mixing for their implication on equivalence principle breaking parameters. The most stringent constraints are from present accelerator neutrino experiments, which are sensitive down to $|\phi|\Delta\gamma \approx 10^{-21}$, atmospheric neutrino experiments, which are sensitive down to $|\phi|\Delta\gamma \approx 10^{-23}$, and solar neutrino experiments, which are sensitive down to $|\phi|\Delta\gamma \approx 10^{-25}$. Currently, the latter two types of measurements actually indicate nonzero neutrino mixing. Assuming that this mixing arises solely from a violation of the equivalence principle, we have analyzed these measurements to find the allowed values of the mixing parameters. A comparison of Figs. 3 and 4(a) shows that the solar and atmospheric neutrino measurements can be simultaneously explained by $\nu_e - \nu_\mu$ mixing with $0.6 < \sin^2 2\theta_G < 0.9$ and $2\times10^{-22} < |\phi\Delta\gamma| < 2\times10^{-21}$. This is an extremely remarkable result since the two types of events are very different in their characteristic neutrino energies and propagation lengths.

Because gravitationally induced mixing has an energy dependence which is the inverse of the mass mixing mechanism, the two mechanisms give quite different predictions. Accelerator neutrino experiments offer a controlled, independent test of the GIM solution. These experiments already rule out the upper half of the parameter region allowed by the solar and atmospheric neutrino data (see Fig. 1). Next generation long-baseline experiments such as MINOS promise to extend these limits by over three orders of magnitude. This solution will also be tested as the next generation of solar and atmospheric neutrino experiments start up in the near future. In particular, the BOREXINO solar neutrino experiment can use long-wavelength vacuum oscillations to directly probe the allowed parameter region, independent of solar model uncertainties.

The test of the equivalence principle discussed in this paper is quite similar to the more familiar tests such as Eötvös-type experiments, Shapiro's time dilation experiments, and others. However, there are theoretical difficulties attendant with a violation of the weak equivalence principle. For instance, it naively suggests the presence of a graviton mass on which there are stringent experimental constraints from data on the bending of light. The importance of this difficulty is not clear since a consistent theory of quantum gravity has proved elusive. Of course, our result certainly does not compel a violation of the equivalence principle. An alternate interpretation might be the existence of a very long-range tensor field, in addition to the gravitational tensor, that couples to electron and muon neutrinos in the manner described here. To distinguish this alternative would require positive indications with particles other than neutrinos—an experimentally challenging task. Neutrinos are uniquely suited for testing the equivalence principle because they are subject to only the two weakest known forces, the weak interactions and gravity.

Experiments currently under construction will decide if the equivalence principle is violated, as the current evidence

suggests. If this parametrization ultimately proves inadequate by more refined experimental results, this type of analysis will reinforce the concept of a geometric theory of gravity. If this class of mechanisms provides the proper parameterization of the data, then perhaps we have at hand the Balmer formula for neutrino oscillations.

ACKNOWLEDGMENTS

A.H. would like to thank Sandip Pakvasa and Xerxes Tata for useful conversations. He would also like to thank the Center for Theoretical Physics of Seoul National University and the Laboratoire de Physique Theorique et Houtes Energies of the University of Paris XI for hospitality during periods of manuscript preparation. Two of the authors (A.H. and J.P.) are also indebted to the Nuclear Theory Institute of the University of Washington for hospitality and stimulating conversation during its 1994 Solar Neutrino Workshop. C.N.L. would like to thank the International School for Advanced Studies, especially S. T. Petcov, for their hospitality during the initial writing of this manuscript. He would also like to thank S. T. Petcov, A. Yu Smirnov, and P. I. Krastev for useful discussions. This work was supported in part by the United States Department of Energy under Grant No. DE-FG02-84ER40163.

[1] J. N. Bahcall and M. M. Pinsonneault, Rev. Mod. Phys. **64**, 885 (1992).
[2] J. N. Bahcall and R. K. Ulrich, Rev. Mod. Phys. **60**, 297 (1989).
[3] S. Turck-Chieze and I. Lopez, Astrophys. J. **408**, 347 (1993); S. Turck-Chieze *et al.*, Phys. Rep. **230**, 57 (1993).
[4] B. M. Pontecorvo, Sov. Phys. JETP **34**, 247 (1958); Z. Maki, M. Nakagawa, and S. Sakata, Prog. Theor. Phys. **28**, 870 (1962).
[5] M. Gasperini, Phys. Rev. D **38**, 2635 (1988); **39**, 3606 (1989).
[6] A. Halprin and C. N. Leung, Phys. Rev. Lett. **67**, 1833 (1991); in *TAUP '91*, Proceedings of the Second International Workshop on Theoretical and Phenomenological Aspects of Underground Physics, Toledo, Spain, edited by A. Morales *et al.* [Nucl. Phys. B (Proc. Suppl.) **28A**, 139 (1992)].
[7] Kamiokande II Collaboration, K. S. Hirata *et al.*, Phys. Lett. B **280**, 146 (1992); see also K. S. Hirata *et al.*, *ibid.* **205**, 416 (1988).
[8] Y. Fukuda *et al.*, Phys. Lett. B **335**, 237 (1994).
[9] IMB Collaboration, R. Becker-Szendy *et al.*, Phys. Rev. D **46**, 3720 (1992); see also D. Casper *et al.*, Phys. Rev. Lett. **66**, 2561 (1991).
[10] Soudan 2 Collaboration, M. Goodman *et al.*, in *Neutrino '94*, Proceedings of the 16th International Conference on Neutrino Physics and Astrophysics, Eilat, Israel, edited by A. Dar, G. Eilam, and M. Gronau [Nucl. Phys. B (Proc. Suppl.) **38**, 227 (1995)].
[11] R. V. Eötvös, Math. Nat. Ber. Ungarn. **8**, 65 (1890); R. V. Eötvös, V. Pekar, and E. Fekete, Ann. Phys. (N.Y.) **68**, 11 (1922).
[12] V. B. Braginsky and V. I. Panov, Sov. Phys. JETP **34**, 463 (1972). For a more recent experiment, see, e.g., B. R. Heckel *et al.*, Phys. Rev. Lett. **63**, 2705 (1989).
[13] I. I. Shapiro, Phys. Rev. Lett. **13**, 789 (1964).
[14] See, e.g., C. M. Will, *Theory and Experiment in Gravitational Physics*, revised ed. (Cambridge University Press, Cambridge, England, 1993).
[15] J. D. Anderson *et al.*, Astrophys. J. **200**, 221 (1975).
[16] M. J. Longo, Phys. Rev. Lett. **60**, 173 (1988).
[17] L. M. Krauss and S. Tremaine, Phys. Rev. Lett. **60**, 176 (1988).
[18] J. M. LoSecco, Phys. Rev D **38**, 3313 (1988).
[19] S. Pakvasa., W. A. Simmons, and T. J. Weiler, Phys. Rev. D **39**, 1761 (1989).
[20] R. Colella, A. W. Overhauser, and S. A. Werner, Phys. Rev. Lett. **34**, 1472 (1975).
[21] See K. Iida, H. Minakata, and O. Yasuda, Mod. Phys. Lett. A **8**, 1037 (1993), for a more detailed discussion.
[22] D. G. Boulware and S. Deser, Ann. Phys. (N.Y.) **89**, 193 (1975).
[23] S. Weinberg, Phys. Rev. **135**, B1049 (1964).
[24] H. Van Dam and M. Veltman, Nucl. Phys. **B22**, 397 (1970).
[25] J. Schwinger, *Particles, Sources, and Fields* (Addison-Wesley Pub. Co., New York, 1988), Vol. I, p. 78.
[26] M. Kenmoku, Y. Okamoto, and K. Shigemoto, Phys. Rev. D **48**, 578 (1993).
[27] See, e.g., Will [14], p. 122.
[28] Gasperini, second reference in Ref. [5].
[29] J. Pantaleone, A. Halprin, and C. N. Leung, Phys. Rev. D **47**, R4199 (1993).
[30] J. N. Bahcall, P. I. Krastev, and C. N. Leung, Phys. Rev. D **52**, 1770 (1995).
[31] H. Minakata and H. Nunokawa, Phys. Rev. D **51**, 6625 (1995).
[32] S. Pakvasa, in *Phenomenology of the Standard Model and Beyond*, Proceedings of the Workshop, Bombay, India, 1989, edited by D. P. Roy and P. Roy (World Scientific, Singapore, 1989), p. 596.
[33] L. Wolfenstein, Phys. Rev. D **17**, 2369 (1978); **20**, 2634 (1979).
[34] T. K. Kuo and J. Pantaleone, Phys. Lett. B **198**, 406 (1987).
[35] P. I. Krastev and S. T. Petcov, Phys. Lett. B **205**, 84 (1988).
[36] R. J. Hughes, Phys. Rev. D **46**, R2283 (1992); M. L. Good, Phys. Rev. **121**, 311 (1961).
[37] M. P. Haugan and T. F. Kauffmann, Phys. Rev. D **52**, 3168 (1995).
[38] P. F. Mende, presented at the International Workshop on Theoretical Physics, Erice, Italy, 1992 (unpublished); T. Damour and A. M. Polyakov, Nucl. Phys. **B423**, 532 (1994).
[39] Particle Data Group, L. Montanet *et al.*, Phys. Rev. D **50**, 1173 (1994).
[40] The constraints on ν_μ-ν_e mixing are derived from L. Borodovsky *et al.*, Phys. Rev. Lett. **68**, 274 (1992) and N. J. Baker *et al.*, *ibid.* **47**, 1576 (1981). The ν_μ-ν_τ and ν_e-ν_τ constraints are derived from N. Ushida *et al.*, *ibid.* **57**, 2897 (1986).
[41] C. Athanassopoulos *et al.*, Phys. Rev. Lett. **75**, 2650 (1995).
[42] J. E. Hill, Phys. Rev. Lett. **75**, 2654 (1995).
[43] R. B. Mann and U. Sarkar, Phys. Rev. Lett. **76**, 865 (1996).
[44] MINOS Collaboration proposal, ''P-875: A Long-baseline

Neutrino Oscillation Experiment at Fermilab,'' Fermilab Report No. NuMI-L-63, 1995 (unpublished); see also the addendum, Report No. NuMI-L-79, 1995 (unpublished).

[45] J. Schneps, in *Neutrino '92*, Proceedings of the XVth International Conference on Neutrino Physics and Astrophysics, Granada, Spain, 1992, edited by A. Morales [Nucl. Phys. B (Proc. Suppl.) **31**, 309 (1993)]; in *Neutrino 94* [10], p. 220; P. Benetti *et al.*, in *TAUP 93*, Proceedings of the Third International Workshop on Theoretical and Phenomenological Aspects of Underground Physics, Assergo, Italy, edited by C. Arpesella *et al.* [Nucl. Phys. B (Proc. Suppl.) **35**, 276 (1994)]; L. K. Resvanis, *ibid.* **35**, 276 (1994); K. Nishikawa *et al.*, ''Proposal for a Long Baseline Neutrino Oscillation Experiment Using KEK-PS and Super-Kamiokande,'' University of Tokyo report, 1995 (unpublished).

[46] R. Davis, D. S. Harmer, and K. C. Hoffman, Phys. Rev. Lett. **20**, 1205 (1968); R. Davis, in *Neutrino '94* [10].

[47] Kamiokande II Collaboration, K. Hirata *et al.*, Phys. Rev. Lett. **65**, 1297 (1990); **65**, 1301 (1990); Phys. Rev. D **44**, 2241 (1991); Y. Suzuki, in *Neutrino '94* [10].

[48] SAGE Collaboration, A. I. Abazov *et al.*, Phys. Rev. Lett. **67**, 3332 (1991); Phys. Lett. B **328**, 234 (1994).

[49] GALLEX Collaboration, P. Anselmann *et al.*, Phys. Lett. B **285**, 376 (1992); **285**, 390 (1992); **327**, 377 (1994).

[50] S. P. Mikheyev and A. Yu Smirnov, Yad. Fiz. **42**, 1441 (1985) [Sov. J. Nucl. Phys. **42**, 913 (1985)]; Nuovo Cimento C **9**, 17 (1986).

[51] T. K. Kuo and J. Pantaleone, Rev. Mod. Phys. **61**, 937 (1989).

[52] N. Hata and P. Langacker, Phys. Rev. D **50**, 632 (1994).

[53] A. Acker, S. Pakvasa, and J. Pantaleone, Phys. Rev. D **43**, R1754 (1991); V. Barger, R. J. N. Phillips, and K. Whisnant, Phys. Rev. Lett. **69**, 3135 (1992); P. I. Krastev and S. T. Petcov, *ibid.* **72**, 1960 (1994).

[54] H. H. Chen, Phys. Rev. Lett. **55**, 1534 (1985); G. T. Ewan *et al.*, Sudbury Neutrino Observatory (SNO) proposal, 1987 (unpublished).

[55] Super Kamiokande Collaboration, Y. Totsuka, Tokyo University Report No. ICRR-227-90-20 (unpublished).

[56] C. Arpesella *et al.*, in *BOREXINO Proposal*, edited by G. Bellini *et al.* (University of Milano, Milano, 1992).

[57] S. Pakvasa and J. Pantaleone, Phys. Rev. Lett. **65**, 2479 (1990).

[58] Y. Z. Qian *et al.*, Phys. Rev. Lett. **71**, 1965 (1993).

[59] S. E. Woosley *et al.*, Astrophys. J. **433**, 229 (1994).

[60] J. Pantaleone, Phys. Lett. B **342**, 250 (1995).

[61] G. Sigl, Phys. Rev. D **51**, 4035 (1995).

[62] D. Harley, T. K. Kuo, and J. Pantaleone, Phys. Rev. D **47**, 4059 (1993); M. Narayan, M. V. N. Murthy, G. Rajasekaran, and S. Uma Sankar, *ibid.* **53**, 2809 (1996).

[63] Ch. Berger *et al.*, Phys. Lett. B **245**, 305 (1990).

[64] R. Becker-Szendy *et al.*, Phys. Rev. Lett. **69**, 1010 (1992).

[65] P. Lipari, M. Lusignoli, and F. Sartogo, Phys. Rev. Lett. **74**, 4384 (1995).

[66] M. Honda, K. Kasahara, and S. Midorikawa, Phys. Lett. B **248**, 193 (1990).

[67] W. Frati, T. K. Gaisser, A. K. Mann, and T. Stanev, Phys. Rev. D **48**, 1140 (1993).

[68] G. L. Fogli and E. Lisi, Phys. Rev. D **52**, 2775 (1995).

[69] P.K.F. Grieder *et al.*, in *Proceedings of the NESTOR Workshop in Pylos, Greece*, edited by L. K. Resvanis (U. Athens, Athens, 1994); S. Barwick *et al.*, Science **267**, 1147 (1995); S. D. Alatin *et al.*, in *TAUP '91* [6], p. 491.

[70] C. W. Misner, K. S. Thorne, and J. A. Wheeler, *Gravitation* (Freeman, San Francisco, 1973).

[71] For the estimate of the potential due to our supercluster, see I. R. Kenyon, Phys. Lett. B **237**, 274 (1990).